Hindawi
Geofluids
Volume 2023, Article ID 7371850, 13 pages
https://doi.org/10.1155/2023/7371850

Research Article

Analytical Solution for Consolidation Behaviors of Combined Composite Foundation Reinforced with Penetrated PCCSs and Floating DM Columns

Chaozhe Zhang,[1,2] **Dingwen Zhang**,[1] **Songyu Liu**,[1] **Jianyong Han**,[3] **Chen Jiang**,[4] **and Yue Zhao**[5]

[1]*Institute of Geotechnical Engineering, School of Transportation, Southeast University, Nanjing 211189, China*
[2]*Department of Civil, Geo and Environmental Engineering, Technical University of Munich, 81245 Munich, Germany*
[3]*School of Civil Engineering, Shandong Jianzhu University, Jinan, Shandong 250101, China*
[4]*Jiangsu Provincial Transportation Engineering Construction Bureau, Nanjing 210004, China*
[5]*Science and Technology Service Platform, Qilu University of Technology (Shandong Academy of Sciences), Jinan, Shandong 250000, China*

Correspondence should be addressed to Dingwen Zhang; zhang@seu.edu.cn

Received 8 October 2022; Revised 1 December 2022; Accepted 28 January 2023; Published 18 February 2023

Academic Editor: Qibin Lin

As the composite pile, the precast concrete piles reinforced with cement-treated soil (PCCS) is formed by driving the precast cement (PC) pile into the deep mixing (DM) column, which has been successfully and widely utilized to support buildings and embankments over soft soil. To increase the pile spacing and give full play to the economic merits of the PCCS, a reinforcement scheme, which involves the combined use of rigid piles and flexible columns, employing penetrated PCCSs and floating DM columns is proposed and utilized for soft soil ground treatment. However, there is a lack of feasible method for consolidation behaviors of this combined composite foundation (CCF) reinforced with penetrated PCCSs and floating DM columns under flexible loads. This paper developed an analytical solution to predict the average consolidation degree of this CCF based on a cylinder consolidation model and double-layer ground consolidation theory. The excess pore pressure and average consolidation degree were calculated by considering the composite pile penetration into the cushion. The analytical method agrees well with results obtained by numerical analysis. Additionally, a parametric study was conducted systematically to analyze the effect of key influence factors on the average consolidation degree of this CCF. The results indicate that the consolidation rate of this CCF can be much faster than that of the natural ground. The consolidation rate strongly depends on the compressive modulus and area replacement ratio of PCCSs. The increasing inner core-outer core modulus ratio and the inner core-subsoil modulus ratio increase the consolidation rate of this CCF. In addition, the consolidation rate increases with the gravel cushion-subsoil modulus ratio, while it decreases with the loading period.

1. Introduction

The composite ground has been widely used in ground improvement due to its convenience and efficiency [1–7]. A variety of pile techniques have been developed to meet various engineering needs, such as stone columns, deep mixing (DM) columns, T-shaped DM columns, jet grouted columns, and precast cement (PC) piles [8–11]. To give full play to merits of different pile techniques, the combined use of multiple pile techniques for soft soil ground improvement was developed [12–15]. Because the combined composite foundation (CCF) can take advantage of multiple performances of every pile technique, it is becoming more well-liked everywhere, but notably in China. [16, 17]. In this CCF system, the piles have different lengths and diameters and use various materials. The common type of the CCF is

the composite ground reinforced by penetrated rigid piles (long piles) and floating flexible or semirigid piles (short piles). In general, the penetrated rigid piles can control the settlements by transferring loads to the deep firm stratum or bearing stratum via piles. The floating columns can improve the bearing capacity of shallow soft soil layers [13].

Similarly, the combination concept of two types of piles also applies to the single pile to form the composite pile, which can exploit both merits. The precast concrete pile reinforced with cement-treated soil (PCCS) is a novel type of composite pile, which is created by driving the PC pile, termed inner core, into the DM column, termed outer core [18–21]. In order to increase the pile spacing and give full play to the economic merits of the PCCS, a novel CCF reinforced by penetrated PCCSs and floating DM columns is proposed and utilized to improve soft soils.

In recent years, the several types of combined composite foundations with reinforcing elements have been proposed, including the PC piles united with lime columns, steel pipe piles united with sand columns, lime columns united with sand columns [22] as well as cement fly-ash gravel (CFG) piles united with lime-soil columns [23]. A comparison of CCFs reinforced by different multiple vertical reinforcement elements was carried out to reveal the bearing mechanism and performance. According to the deformation consistency of pile-soil and the bilinear elastoplastic model of the soil, Zheng et al. [24] proposed the analytical solution for the CCF under elastic and plastic circumstances to calculate the composite modulus accurately and built a design method for the multicolumn composite foundation with DM columns united with stone columns [25].

The bearing performances of the PCCS were investigated by means of experimental, theoretical, and numerical analysis under vertical and lateral loads [26–31]. The inner core is installed to bear external loads, while the outer core can increase the shaft friction of the inner core and effectively transfer the inner core's axial force to the surrounding soil [18]. The PCCS can reduce costs by nearly 30% under the same bearing capacity provided by the PCCS and the piles with the same geometric dimensioning [32]. Wang et al. [20] developed a practical analytical approach for predicting the bearing capacity of the PCCS considering the pile-soil interaction and nonhomogeneity of subsoil shear. Wang et al. [19] proposed a modified p-y curve model to calculate the lateral bearing capacity of the PCCS based on field tests of the PCCSs and indicated that cemented soil could reduce the bending moment and lateral deflections. Based on tested results, Wang et al. [33] found that the stiffened deep mixing (SDM) column-supported embankment could significantly reduce the postconstruction settlement by 27.3%-68.3 compared to the conventional DM column-reinforced composite foundation. Ye et al. [26] established a series of finite element (FE) models to analyze the bearing mechanism of the SDM column-supported embankment.

In addition, several methodologies consist of the field-scale tests, numerical analysis as well as analytical solutions for studying the consolidation behaviors of the composite foundations reinforced by different vertical elements. Because of the accuracy and convenience for end-users, analytical solutions are more popular than field measurement and numerical methods [16, 34, 35]. Considerable achievements on the consolidation of the permeable column- and impermeable pile-reinforced composite foundations which adopted Biot's consolidation theory have been obtained [13, 36, 37]. As for the granular column-improved composite grounds under various time-dependent loading, many analytical solutions have been proposed considering well resistance, smear effect, consolidation of stone columns, and several types of drained boundary [38–42]. The analytical methods for consolidation behaviors of impermeable pile-improved soft grounds also have been developed considering floating and penetrated piles, piercing into the gravel cushion, a partial drained boundary as well as the varying vertical stress increment with depth in subsoils [2, 3, 9]. In addition, the consolidation behaviors of the CCF improved by cohesive piles with prefabricated vertical drains have been investigated. Lu et al. [16] presented two analytical models of the composite foundation improved with impervious columns and vertical drains under different distribution modes. However, there are limited research on the consolidation of the CCF with multiple types of piles. Abusharar et al. [43] studied the consolidation of a CCF with CFG piles united with lime columns under embankment load and found that this CCF can increase the consolidation rate and embankment stability. Yang et al. [13] proposed a theoretical method of the CCF improved by impervious long piles and impervious short DM columns. Since, the CCF reinforced by penetrated PCCSs and floating DM columns is a novel technique, whose consolidation behaviors need further research.

The main purpose of this work is to propose an analytical solution for consolidation of the CCF reinforced with penetrated PCCSs and floating DM columns, which is simplified as a double-layered consolidation foundation based on a quasiequal-strain assumption [44]. The analytical solution of the average consolidation degree of this CCF is derived by the boundary conditions of vertical additional stress increment linearly with depth in subsoils. Moreover, the proposed analytical method is validated by numerical analysis. A sensitive analysis is conducted to describe the key influence factors on the consolidation behaviors of this CCF.

2. Mathematical Model

2.1. Model Description and Basic Assumptions. The penetrated PCCSs as the long piles and floating DM columns as the short columns can be arranged in four types of distribution modes, including triangular, intensive triangular, rectangular, and intensive rectangular distributions, as shown in Figure 1. The primary step in analyzing the consolidation behaviors is partitioning this multipile composite ground into the square unit cells. The unit cell is adopted as the representative of the CCP and converted into a cylindrical unit cell using based on equivalent hypothesize of the sectional area [16, 17]. In general, the unit cell can be adopted in two patterns: (1) *Form* A is a PCCS at the center with N DM columns dispersed separately at its boundary and (2) *Form* B is a DM column at the center with N PCCSs distributed separately at its perimeter. The cross-sectional area of

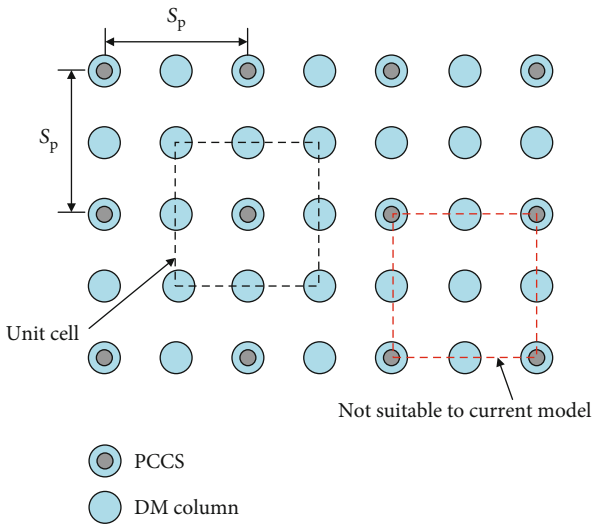

Figure 1: Layout of this CCF reinforced with penetrated PCCSs and floating DM columns.

each PCCS distributed independently at its boundary within the unit cell makes up the value of N. With respect to triangular and rectangular distribution patterns, selecting any pile at the center for the consolidation path in the subsoil is constant, since the PCCS and DM columns can be regarded as impervious piles. However, for the intensive rectangular distribution patterns, it is necessary to select the PCCS located at the center. Otherwise, it makes the problem more complex when other DM columns are distributed at the circumferential boundary. Therefore, *Form* B is adopted in this paper to analyze the cases of rectangular and intensive rectangular distributions.

In the current study, the penetrated PCCS with a long inner core as the long pile and the floating DM column as the short column is installed in a rectangular mode with identical center-to-center spacing of S_p. This penetrated PCCS penetrates the whole soft soil layers seated on an impermeable bearing layer in this composite ground, and one PCCS at the center and eight DM columns are distributed at the boundary, where the value of N is 3. Figure 2 presents the cylinder model with an equal cross-sectional area transferred from the unit cell. Its simplified model comprises two improved areas according to the cross-section of DM column, which are named Region A and Region B with the permeability coefficient (k_{v1} and k_{v2}), compressive modulus (E_{s1} and E_{s2}), consolidation coefficient (c_{v1} and c_{v2}), and length (h_1 and h_2), respectively. r_{dm} and r_{pc} are the radius of the PC pile and the DM column, respectively. E_{dm} and E_{pc} are the compressive modulus of the concrete and the cemented soil, respectively. r_n is the radius of the unit cell, and r_e is the outside radius of the simplified model of the CCF, which can be determined as follows:

$$\begin{aligned} r_e^2 &= r_n^2 - N r_{dm}^2, \\ \frac{\pi}{4} r_n^2 &= S_p^2. \end{aligned} \tag{1}$$

The reinforced gravel cushion laying on the piles and surrounding soil is subjected to a ramp load, $p(t)$. Water flow is prohibited across the bottom and lateral surfaces of the model due to the underlying impermeable layer, whilst is allowed across the ground surface to analyze the single drainage of the CCF.

The following assumptions during the analysis in this paper are given below:

(i) Darcy's law is obeyed for the seepage of the water in the surrounding soil. k_{v1}, k_{v2}, E_{s1}, and E_{s2} are assumed to remain constant. The subsoils are regarded as fully saturated state

(ii) PC piles and DM columns are assumed to be impervious, where no flow and the consolidation occur at the PC pile-DM column interface and DM column-soil interface

(iii) There is no interface slip between the PC pile-cemented soil of the PCCS

(iv) It is considered that the vertical strains of the DM column and its surrounding soil are equal at any depth

(v) A quasiequal strain assumption is used between the PCCS and its surrounding soil due to the pile top pierced into the gravel cushion to generate the relatively large penetration, δ_1 [45]. The deformation of the surrounding soil is relatively close to the total of the pile shaft compression and the pile head penetration value. Since the pile tip is located on a firm soil layer, the pile tip piercing into the underlying soil layer is not taken into account. Therefore, the volumetric strain, ε_v, can be obtained as follows:

$$\varepsilon_v = \frac{\bar{\sigma}_{pc}}{E_{pc}} + \frac{\delta_1}{h_1} = \frac{\bar{\sigma}_{dm1}}{E_{dm}} + \frac{\delta_1}{h_1} = \frac{\bar{\sigma}_{dm2}}{E_{dm}} = \frac{\bar{\sigma}_{s1} - \bar{u}_1}{E_{s1}}, \tag{2}$$

$$\delta_1 = \frac{\pi\left(1 - \mu_c^2\right) p_{ac} r_p}{2E_c}, \tag{3}$$

where $\bar{\sigma}_{pc}$, $\bar{\sigma}_{dm1}$, and $\bar{\sigma}_{dm2}$ are the vertical stress of inner core and outer core of the PCCS as well as the DM column, respectively. $\bar{\sigma}_{s1}$ and $\bar{u}_{s1}$ are the vertical stress and the excess pore pressure of the soil around piles in Region A, respectively. p_{ac}, μ_c, and E_c are the vertical stress of the pile top, the Poisson's ratio, and the compressive modulus of the cushion, respectively.

Substituting Equation (3) into Equation (2) yields

$$\varepsilon_v = \frac{\bar{\sigma}_{pc}}{E_{epc}} = \frac{\bar{\sigma}_{dm1}}{E_{edm}} = \frac{\bar{\sigma}_{dm2}}{E_{dm}} = \frac{\bar{\sigma}_{s1} - \bar{u}_1}{E_{s1}}, \tag{4}$$

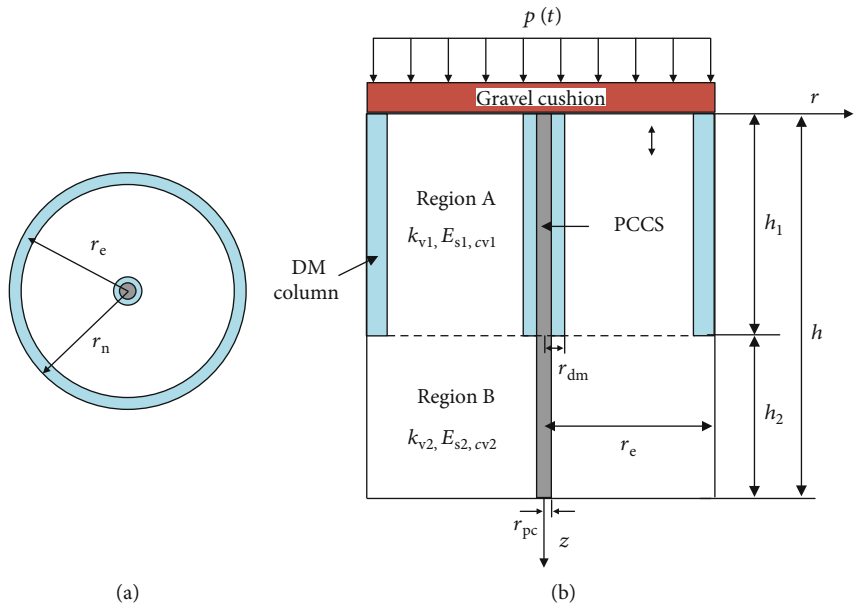

Figure 2: Schematic diagram of consolidation model; (a) plan view; (b) elevation plan.

where E_{epc} and E_{edm} are the equivalent compressive moduli of PC pile and DM column of the PCCS:

$$E_{epc} = \frac{2h_1E_cE_{pc}}{2h_1E_c + \pi(1-\mu_c^2)E_{pc}r_{sp}},$$
$$E_{edm} = \frac{2h_1E_cE_{dm}}{2h_1E_c + \pi(1-\mu_c^2)E_{dm}r_{dm}}. \quad (5)$$

2.2. Governing Equation

2.2.1. Consolidation Equation for the Subsoil in Region A. In the axisymmetric consolidation model, the average vertical stress in Region A within the CCF is transferred from the cushion to the DM columns, the PCCSs, and the soil around piles. $\sigma(t,z)$ is the average total stress in this CCF induced by the external load, $p(t)$. The equilibrium equation at any depth in Region A can be written as follows:

$$(1-m_1-m_2)\bar{\sigma}_{s1} + m_1\left[(1-\rho)\bar{\sigma}_{dm1} + \rho\bar{\sigma}_{pc}\right] + m_2\bar{\sigma}_{dm2} = \sigma(t,z), \quad (6)$$

where m_1 and m_2 are the area replacement ratios of the PCCS and DM column, respectively, and ρ is the ratio between the inner and outer cores' cross-sectional areas.

From Equation (4) and Equation (6), the vertical volumetric strain of the PCCSs, DM columns, and the subsoil at any depth, ε_v, can be expressed as follows:

$$\varepsilon_v = \frac{\sigma(t,z) - (1-m_1-m_2)\bar{u}_{s1}}{E_{comp1}}, \quad (7)$$

$$E_{comp1} = m_1\left[(1-\rho)E_{edm} + \rho E_{epc}\right] + m_2E_{dm} + (1-m_1-m_2)E_{s1}, \quad (8)$$

where E_{comp1} is the composite compressive modulus of this CCF in Region A.

From Equation (7), the time derivative of ε_v of this CCF can be obtained as follows:

$$\frac{\partial\varepsilon_v}{\partial t} = -\frac{(1-m_1-m_2)}{E_{comp1}}\frac{\partial\bar{u}_{s1}}{\partial t} + \frac{1}{E_{comp1}}\frac{\partial\sigma(t,z)}{\partial t}. \quad (9)$$

The vertical flow of the pore water of the surrounding soil is permitted in the impervious column reinforced ground; the consolidation equation of the subsoil in Region A can be written as follows:

$$\frac{\partial\varepsilon_v}{\partial t} = -\frac{k_{v1}}{\gamma_w}\frac{\partial^2\bar{u}_{s1}}{\partial z^2}. \quad (10)$$

By substituting Equation (9) into Equation (10), the governing differential equation for the consolidation for the subsoil in Region A can be derived:

$$\frac{\partial\bar{u}_{s1}}{\partial t} = \frac{k_{v1}E_{comp1}}{(1-m_1-m_2)\gamma_w}\frac{\partial^2\bar{u}_{s1}}{\partial z^2} + \frac{1}{(1-m_1-m_2)}\frac{\partial\sigma(t,z)}{\partial t}. \quad (11)$$

A simplified version of Equation (11) can be rearranged as follows:

$$\frac{\partial\bar{u}_{s1}}{\partial t} = c_{v1e}\frac{\partial^2\bar{u}_{s1}}{\partial z^2} + \frac{1}{(1-m_1-m_2)}\frac{\partial\sigma(t,z)}{\partial t},$$
$$c_{v1e} = \frac{E_{compl}k_{v1}}{(1-m_1-m_2)\gamma_w} = \left[1 + \frac{m_1\left[(1-\rho)E_{edm} + \rho E_{epc}\right] + m_2E_{dm2}}{(1-m_1-m_2)E_{s1}}\right]c_{v1}, \quad (12)$$

where c_{v1e} is defined as the equivalent vertical consolidation coefficient of the subsoil in Region A.

2.2.2. Consolidation Equation for the Subsoil in Region B. From the equilibrium equation of the PCCS and the soil around the inner core in Region B, the following relation can be obtained:

$$(1 - m_1\rho)\bar{\sigma}_{s2} + m_1\rho\bar{\sigma}_{pc} = \sigma(t, z), \tag{13}$$

where $\bar{\sigma}_{s2}$ is the vertical stress of d the soil around the inner core in Region B.

Similarly, ε_v for the inner core of the PCCS and its surrounding soil in Region B, can be written as follows:

$$\varepsilon_v = \frac{\bar{\sigma}_{pc}}{E_{pc}} = \frac{\bar{\sigma}_{s2} - \bar{u}_{s2}}{E_{s2}}, \tag{14}$$

where $\bar{u}_{s2}$ is the average excess pore pressure of the soil around the inner core in Region B.

Combining Equation (13) and Equation (14) yeilds

$$\varepsilon_v = \frac{\sigma(t, z) - (1 - m_1\rho)\bar{u}_{s2}}{E_{comp2}}, \tag{15}$$

$$E_{comp2} = (1 - m_1\rho)E_{s2} + m_1\rho E_{pc}, \tag{16}$$

where E_{comp2} is the composite compressive modulus of this CCF in Region B.

It can be derived by taking the time derivative of ε_v that

$$\frac{\partial\varepsilon_v}{\partial t} = -\frac{(1 - m_1\rho)}{E_{comp2}}\frac{\partial\bar{u}_{s2}}{\partial t} + \frac{1}{E_{comp2}}\frac{\partial\sigma(t, z)}{\partial t}. \tag{17}$$

Similar to the derivation of Equation (10), the consolidation equation of this CCF in Region B can be obtained:

$$\frac{\partial\varepsilon_v}{\partial t} = -\frac{k_{v2}}{\gamma_w}\frac{\partial^2\bar{u}_{s2}}{\partial z^2}. \tag{18}$$

From Equation (17) and Equation (18), the governing equation for the consolidation of the subsoil in Region B can be derived:

$$\frac{\partial\bar{u}_{s2}}{\partial t} = c_{v2e}\frac{\partial^2\bar{u}_{s2}}{\partial z^2} + \frac{1}{(1 - m_1\rho)}\frac{\partial\sigma(t, z)}{\partial t}, \tag{19}$$

where c_{v2e} is the equivalent vertical consolidation coefficient of the subsoil in Region B, considering the effect of the inner core of the PCCS:

$$c_{v2e} = \frac{k_{v2}E_{comp2}}{(1 - m_1\rho)\gamma_w} = \left[1 + \frac{m_1\rho E_{pc}}{(1 - m_1\rho)E_{s2}}\right]c_{v2}. \tag{20}$$

3. Analytical Solutions

Equation (21) with c_{v1e} and c_{v2e} is similar with the governing equations provided by Xie [44] in format. Based on the above derivation, this CCF reinforced with penetrated PCCSs and floating DM columns can be regarded as a double-layered ground.

$$\begin{cases} \dfrac{\partial\bar{u}_{s1}}{\partial t} = c_{v1e}\dfrac{\partial^2\bar{u}_{s1}}{\partial z^2} + \dfrac{1}{(1 - m_1 - m_2)}\dfrac{\partial\sigma(t, z)}{\partial t}, \\ \dfrac{\partial\bar{u}_{s2}}{\partial t} = c_{v2e}\dfrac{\partial^2\bar{u}_{s2}}{\partial z^2} + \dfrac{1}{(1 - m_1\rho)}\dfrac{\partial\sigma(t, z)}{\partial t}. \end{cases} \tag{21}$$

3.1. Boundary Conditions. Since this CCF with the top previous surface and the bottom impervious surface, the boundary conditions of this consolidation model are as follows:

$$\begin{cases} \bar{u}_{s1}(t, z) = 0, & z = 0, \\ \dfrac{\partial\bar{u}_{s2}(t, z)}{\partial z} = 0, & z = h. \end{cases} \tag{22}$$

Equation (23) can be derived by expressing Equation (6) and Equation (13) based on the principle of effective stress.

$$\begin{aligned}(1 - m_1 - m_2)(\bar{\sigma}_{s1} - \bar{u}_{s1}) + m_1\left[(1 - \rho)\bar{\sigma}_{dm1} + \rho\bar{\sigma}_{pc}\right] + m_2\bar{\sigma}_{dm2} \\ = (1 - m_1\rho)(\bar{\sigma}_{s2} - \bar{u}_{s2}) + m_1\rho\bar{\sigma}_{pc}.\end{aligned} \tag{23}$$

According to Equations (6), (13), and (23), the continuity conditions of the boundary pore pressure can be obtained as follows:

$$(1 - m_1 - m_2)\bar{u}_{s1} = (1 - m_1\rho)\bar{u}_{s2}. \tag{24}$$

Based on the continuous condition of seepage on the Region A-Region B interface, the following relation can be obtained:

$$(1 - m_1 - m_2)k_{v1}\frac{\partial\bar{u}_{s1}}{\partial z} = (1 - m_1\rho)k_{v2}\frac{\partial\bar{u}_{s2}}{\partial z}. \tag{25}$$

From Equations (7) and (15), the excess pore water pressure at initial time can be obtained:

$$t = 0 : \begin{cases} \bar{u}_{s1} = \dfrac{\sigma(t, z)}{1 - m_1 - m_2}, \\ \bar{u}_{s2} = \dfrac{\sigma(t, z)}{1 - m_1\rho}. \end{cases} \tag{26}$$

As shown in Figure 3, this CCF is subjected to a ramp load, which increases with time until t_u, and then remains a constant value, p_u. The additional stress distribution of

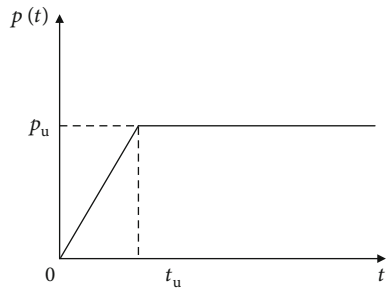

Figure 3: Relationship between load and time.

this CCF resulting from p_u assumed to vary linearly along the depth as shown in Figure 4 can be expressed as follows:

$$\sigma(t,z)=\begin{cases}\dfrac{\sigma_0(h-z)t}{ht_u}, & t<t_u,\\ \dfrac{\sigma_0(h-z)}{h}, & t\geq t_u,\end{cases} \tag{27}$$

where σ_0 is the vertical stress of the ground surface.

3.2. Derivation of Pore Pressure and Consolidation Degree under Ramp Loading. In this paper, a, b, and c as the dimensionless parameters are adopted to simplify the derivation as follows:

$$\begin{cases} a=\dfrac{k_{v2}}{k_{v1}},\\ b=\dfrac{E_{comp1}(1-m_1\rho)}{E_{comp2}(1-m_1-m_2)},\\ c=\dfrac{h_2}{h_1}.\end{cases} \tag{28}$$

Based on the consolidation model of double-layered ground under ramp loading, the governing equations of the composite ground can be solved:

$$\bar{u}_{s1}=\sum_{m=1}^{\infty}\sin\left(\frac{\lambda_m z}{H_1}\right)e^{-\beta_m t}C_m T_m(t), \tag{29}$$

$$\bar{u}_{s2}=\sum_{m=1}^{\infty}A_m\cos\left(\mu\lambda_m\frac{h-z}{h_1}\right)e^{-\beta_m t}C_m T_m(t), \tag{30}$$

where A_m, C_m, λ_m, and β_m are unknown coefficients and $T_m(t)$ is the pending function united with the external load.

According to the boundary condition of the initial stress and water flow, the above-mentioned parameters can be obtained as follows:

$$A_m=\frac{\sin\lambda_m}{\cos(\mu c\lambda_m)}, \tag{31}$$

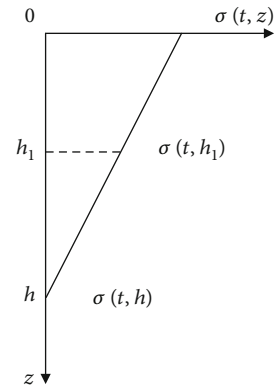

Figure 4: Relationship between of the additional stress and depth.

$$\beta_m=\frac{c_{v1e}\lambda_m^2}{h_1^2}, \tag{32}$$

$$C_m=\frac{2}{\lambda_m\left(1+bcA_m^2\right)}, \tag{33}$$

$$\mu=\sqrt{\frac{c_{v1e}}{c_{v2e}}}, \tag{34}$$

$$\sqrt{ab}\sin\lambda_m\sin(\mu c\lambda_m)=\cos\lambda_m\cos(\mu c\lambda_m). \tag{35}$$

The eigenvalues λ_m are the root of the eigen-Equation (35). From Equation (29), Equation (30), and Equation (21), the pending function of $T_m(t)$ can be calculated by

$$\begin{cases} T_m=\dfrac{1}{1-m_1-m_2}\dfrac{\sigma_u}{t_u}\displaystyle\int_0^t e^{\beta_m t}dt, & 0<z\leq h_1,\\ T_m=\dfrac{1}{1-m_1\rho}\dfrac{\sigma_u}{t_u}\displaystyle\int_0^t e^{\beta_m t}dt, & h_1<z\leq h.\end{cases} \tag{36}$$

Substituting Equations (31)–(35) to Equation (29) and Equation (30), the average excess pore water pressure of this CCF reinforced with penetrated PCCSs and floating DM columns in Region A ($\bar{u}_1$) and in Region B ($\bar{u}_2$) can be derived during $0\leq t<t_u$.

$$\begin{cases} \bar{u}_{s1}=\dfrac{\sigma_u}{1-m_1-m_2}\displaystyle\sum_{m=1}^{\infty}\frac{C_m}{\lambda_m^2 T_{vtu}}\sin\left(\frac{\lambda_m z}{h_1}\right)\left(1-e^{-\lambda_m^2 T_{v1}}\right),\\ \bar{u}_{s2}=\dfrac{\sigma_u}{1-m_1\rho}\displaystyle\sum_{m=1}^{\infty}\frac{A_m C_m}{\lambda_m^2 T_{vtu}}\cos\left(\mu\lambda_m\frac{h-z}{h_1}\right)\left(1-e^{-\lambda_m^2 T_{v1}}\right),\end{cases} \tag{37}$$

where T_{vtu} is the time factor when t equals to t_u and T_{v1} is the time function, which can be obtained as

$$\begin{cases} Tvtu=\dfrac{c_{v1e}t_u}{h_1^2},\\ Tv1=\dfrac{c_{v1e}t}{h_1^2}.\end{cases} \tag{38}$$

Furthermore, the functions of $\bar{u}_1$ of this CCF for $t > t_c$ can be derived as

$$\begin{cases} \bar{u}_{s1} = \dfrac{\sigma_u}{1-m_1-m_2}\displaystyle\sum_{m=1}^{\infty}\dfrac{C_m}{\lambda_m^2 T_{vtu}}\sin\left(\dfrac{\lambda_m z}{h_1}\right)e^{-\lambda_m^2 T_{v1}}\left(e^{\lambda_m^2 T_{vtu}}-1\right), \\ \bar{u}_{s2} = \dfrac{\sigma_u}{1-m_1\rho}\displaystyle\sum_{m=1}^{\infty}\dfrac{A_m C_m}{\lambda_m^2 T_{vtu}}\cos\left(\mu\lambda_m\dfrac{h-z}{h_1}\right)e^{-\lambda_m^2 T_{v1}}\left(e^{\lambda_m^2 T_{vtu}}-1\right). \end{cases} \tag{39}$$

In this study, the average consolidation degree of this CCF concerning the settlement, U_s, can be written as follows:

$$U_s(t) = \frac{1/E_{s1}\int_0^{h_1}(\bar{\sigma}_{s1}-\bar{u}_{s1})dz + (1/E_{s2})\int_{h_1}^{h}(\bar{\sigma}_{s2}-\bar{u}_{s2})dz}{1/E_{s1}\int_0^{h_1}\bar{\sigma}_{s1u}(z)dz + (1/E_{s2})\int_{h_1}^{h}\bar{\sigma}_{s2u}(z)dz}, \tag{40}$$

where $\bar{\sigma}_{s1u}$ and $\bar{\sigma}_{s2u}$ are the final stress of the soil in Region A and Region B, respectively.

Combining Equation (4) and Equation (6), the vertical stress of the surrounding soil in Region A can be obtained:

$$\bar{\sigma}_{s1} = \frac{\sigma(t,z) + \left[m_1(1-\rho)Y_{dm} + m_1\rho Y_{pc} + m_2 Y_{dm2}\right]\bar{u}_{s1}}{(1-m_1-m_2) + m_1\left[(1-\rho)Y_{dm} + \rho Y_{pc}\right] + m_2 Y_{dm2}}. \tag{41}$$

From Equation (41), $\bar{\sigma}_{s1u}$ can be derived:

$$\bar{\sigma}_{s1u} = \frac{\sigma(t,z)}{\left\{(1-m_1-m_2) + m_1\left[(1-\rho)Y_{dm} + \rho Y_{pc}\right] + m_2 Y_{dm2}\right\}}, \tag{42}$$

where Y_{dm} and Y_{pc} are the dimensionless parameters, which can be expressed by

$$Y_{dm} = \frac{E_{edm}}{E_{s1}}\ ;\ Y_{dm2} = \frac{E_{dm}}{E_{s1}}\ ;\ Y_{pc} = \frac{E_{epc}}{E_{s1}}. \tag{43}$$

Similarly, combining Equation (4) and Equation (13), the average and final stresses of the soil in Region B can be obtained:

$$\bar{\sigma}_{s2} = \frac{\sigma(t,z) + m_1\rho Y_{pc2}\bar{u}_{s2}}{1-m_1\rho + m_1\rho Y_{pc2}}, \tag{44}$$

$$\bar{\sigma}_{s2u} = \frac{\sigma(t,z)}{1-m_1\rho + m_1\rho Y_{pc2}}, \tag{45}$$

where $Y_{pc2} = E_{pc}/E_{s2}$.

Substituting Equations (37)–(39) and Equations (41)–(45) into Equation (40), the overall average consolidation degree of this CCF during $0 \le t < t_u$ can be obtained:

$$U(t) = \frac{t_u}{t} - \frac{2hh_1}{T_{vtc}}\frac{m_{v1e}\sum_{m=1}^{\infty}C_m\left(1-e^{-\lambda_m^2 T_{v1}}\right)/\lambda_m^3(\cos\lambda_m - 1) - m_{v2e}\sum_{m=1}^{\infty}A_m C_m\left(1-e^{-\lambda_m^2 T_{v1}}\right)/\mu\lambda_m^3\sin\mu\lambda_m(h-h_1)/h_1}{m_{v1e}\left(h_1^2-2h_1h\right) + m_{v2e}(h-h_1)^2}. \tag{46}$$

Similarly, $U(t)$ of the CCF during $t \ge t_u$ can be derived as

$$U(t) = 1 + \frac{2hh_1}{T_{vtc}}\frac{m_{v1e}\sum_{m=1}^{\infty}C_m e^{-\lambda_m^2 T_{v1}}\left(e^{\lambda_m^2 T_{vtc}}-1\right)/\lambda_m^3(\cos\lambda_m - 1) - m_{v2e}\sum_{m=1}^{\infty}A_m C_m e^{-\lambda_m^2 T_{v1}}\left(e^{\lambda_m^2 T_{vtc}}-1\right)/\mu\lambda_m^3\sin\mu\lambda_m(h-h_1)/h_1}{m_{v1e}\left(h_1^2-2h_1h\right) + m_{v2e}(h-h_1)^2},$$

$$\begin{cases} m_{v1e} = \dfrac{1}{E_{s1e}} = \dfrac{1}{\left\{\left[(1-m_1-m_2) + m_1\left[(1-\rho)Y_{dm} + \rho Y_{pc}\right] + m_2 Y_{dm2}\right]E_{s1}\right\}}, \\ m_{v2e} = \dfrac{1}{E_{s2e}} = \dfrac{1}{\left\{\left[1-m_1\rho + m_1\rho Y_{pc2}\right]E_{s2}\right\}}, \end{cases} \tag{47}$$

where m_{v1e} and m_{v2e} are the volume compressibility equivalent coefficients of the surrounding soil in Region A and Region B, respectively.

3.3. Model Calibration. Numerical analysis using Plaxis 3D (2016) was carried out to verify the accuracy of the current analytical solution for this CCF. A cubic model (height = 20 m and pile spacing of PCCSs = 4 m) is adopted for numerical simulation, as shown in Figure 5. The penetrated PCCS as the long pile consisted of the outer core with a length of 12 m and the inner core with a length of 20 m. The floating DM column is regarded as the short pile with a length of 12 m. The diameter of the outer core and the DM column is 800 mm, while the diameter of the inner core is 400 mm. m_1 and m_2 are 0.15 and 0.09, respectively. A 0.3 m thickness gravel cushion is seated on the surface of this CCF. After the completion of initial geostatic stress balance, a ramp uniform external load $p_u = 100$ kPa is applied linearly on the gravel cushion within 60 days ($t_u = 60$ d), followed by consolidation of 1000 days.

Mohr-Coulomb (MC) model is adopted to express the elastic-perfectly plastic behaviors of the DM column, subsoil, and gravel cushion, while concrete is regarded as isotropic linear-elastic material. The Young's modulus, E, of every material can be obtained from using the equation $E = E_s(1 + \nu)(1 + 2\nu)/(1 - \nu)$, where E_s and ν are the constrained modulus and Poisson's ratio of the material, respectively. Table 1 presents the primary material parameters. A 10-node tetrahedral cell is used to model the pile, DC column, soil, and gravel cushion.

Regarding the drainage boundary condition, the lateral and bottom surfaces are regarded as impermeable surfaces, while the water flow is permitted through the ground surface. The friction coefficients of DM column-soil and inner-outer cores of the PCCS are 0.1 (Brinkgreve et al., 2008) and 0.4 [28, 29], respectively.

Figure 6 presents the comparison of $U(t)$ of this CCF obtained from the current analytical method and FE model. It indicates that the consolidation rate obtained from numerical simulation agrees well with that predicted by the current analytical method. However, the theoretical values are slightly bigger than the numerical ones for $t > t_u$. The main reason is that the nonlinear variation of the additional stress of subsoils in the numerical analysis is different from that assumed to vary linearly along with the depth in the analytical method.

4. Parametric Study of This CCF

A parametrical study is conducted to study the consolidation behaviors of the CCF reinforced with penetrated PCCSs and floating DM columns. In this analysis, the real time is replaced by a dimensionless time factor $T_v = c_{v1}t/h$. The effect of seven key influence factors on consolidation behaviors of this CCF is analyzed. All the parameters of the FE model are adopted for the baseline unit cell.

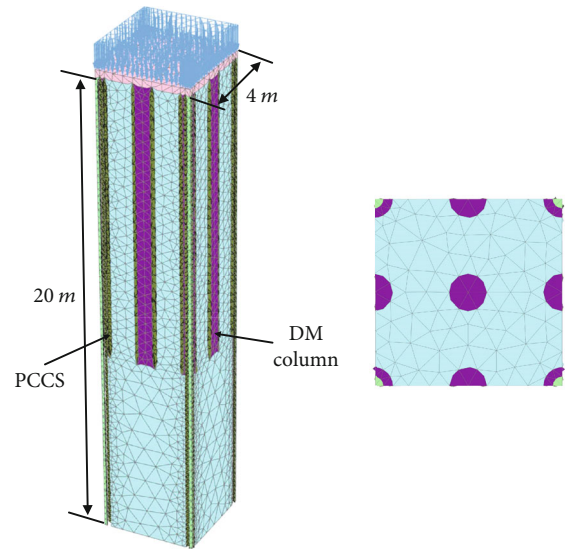

Figure 5: Finite element model.

4.1. Effect of m_1. Figure 7 depicts the average degree of consolidation, U_s versus time factor T_v for m_1. It can be seen from Figure 7 that the consolidation rate increases with m_1 for the constant m_2. This appears to be only effective up to a certain value of m_1, resulting from that the larger m_1, the smaller the reinforcement zone of the pile and the shorter the pore water seepage path of the soil around piles.

4.2. Effect of m_2. The average degree of consolidation U_s versus time factor T_v for varying m_2 in Figure 8 considers the two cases that (L_{dm}/L_{pc}) are 0.3 and 0.6. The consolidation rate slightly increases with m_2 varying from 0.09 to 0.18. Compared with m_1, DM columns have inapparent influence on the consolidation rate of this CCF with penetrated PCCSs and floating DM columns. Besides, the effect on consolidation rate of the CCF with L_{dm}/L_{pc} of 0.6 is relatively significant than that of the CCF with L_{dm}/L_{pc} of 0.3, which is attributed to the floating effect of the DM columns.

4.3. Effect of E_{pc}/E_{dm}. Figure 9 presents the effect of inner core-outer core modulus ratio (E_{pc}/E_{dm}) on consolidation behavior of CCFs. E_{dm} includes 0, 150 MPa, 200 MPa, 300 MPa, and 600 MPa, keeping E_{pc} as 30 GPa. When the value of E_{dm} is assigned to zero, the CCF reinforced with penetrated PCCSs and DM columns degenerated to the CCF improved by PC piles united with DM columns. Figure 9 indicates that the average consolidation rate increases with E_{pc}/E_{dm} and the equivalent consolidation coefficient increases with E_{dm}. Moreover, compared with the traditional the CCF improved by PC piles united with DM columns, the consolidation rate of the CCF improved by penetrated PCCSs increases obviously, implying that the outer core can accelerate the consolidation rate of this CCF to some extent.

Table 1: Parameters in the numerical simulation.

Material	Unit weight, γ (kN/m^3)	Compression modulus, E_s (MPa)	Effective cohesion, c' (kPa)	Effective friction angle, φ' (°)	ν	Permeability coefficient, k_v (m/s)
Soft soil	18	3	4	18	0.4	1×10^{-8}
Gravel cushion	19	30	0	32	0.3	—
Cemented soil	20	150	500	36	0.3	—
Concrete	24	20000	—	—	0.20	—

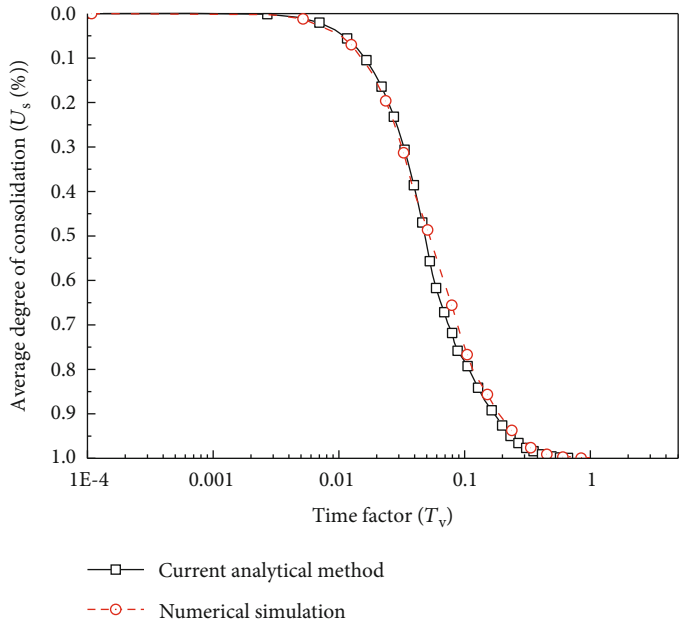

Figure 6: Comparison of the current analytical solution and numerical analysis.

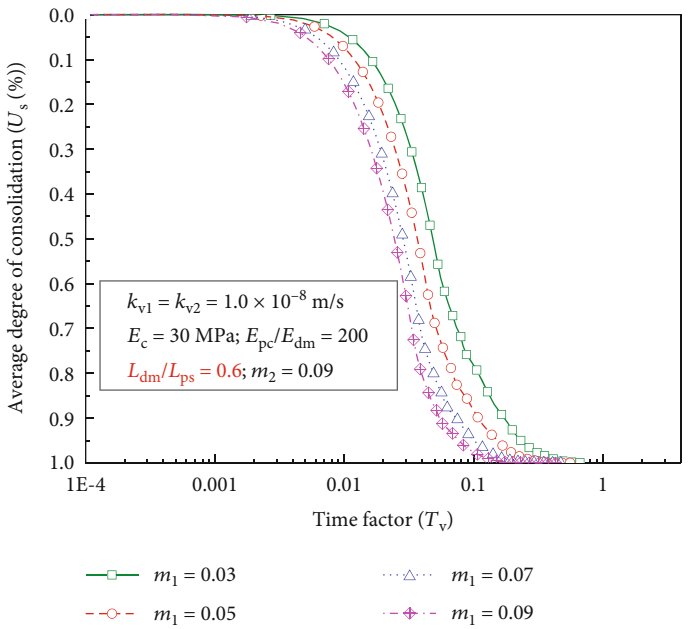

Figure 7: Effect of m_1 on the consolidation rate.

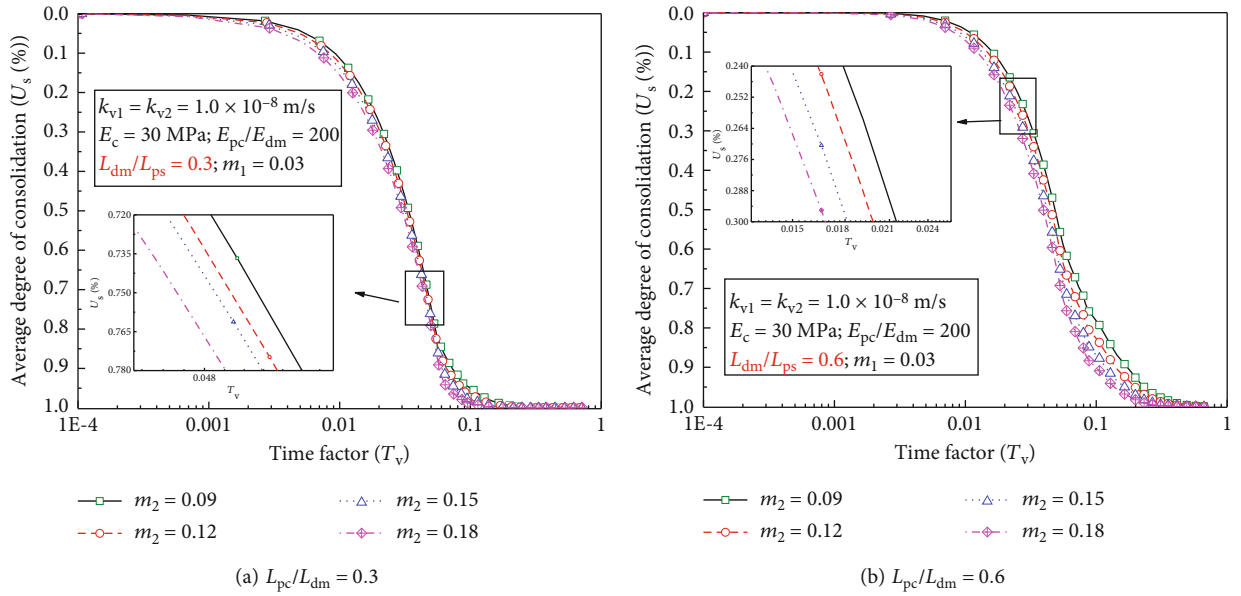

(a) $L_{pc}/L_{dm} = 0.3$ (b) $L_{pc}/L_{dm} = 0.6$

Figure 8: Effect of m_2 on the consolidation rate.

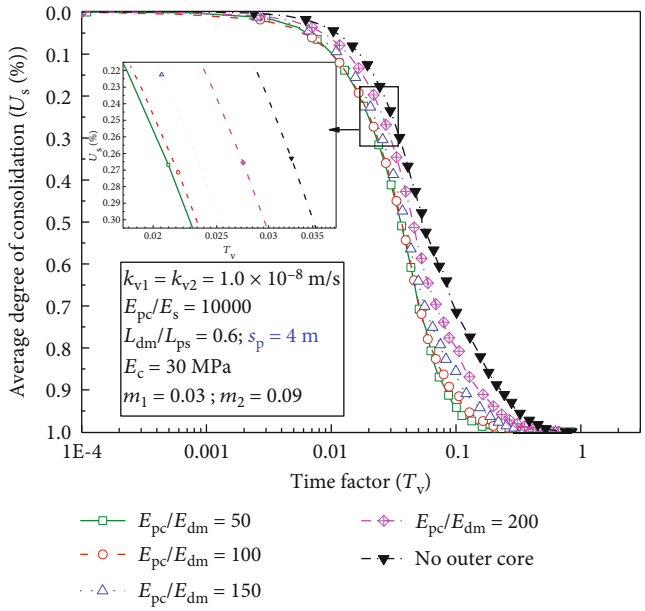

Figure 9: Effect of E_{pc}/E_{dm} on the consolidation rate.

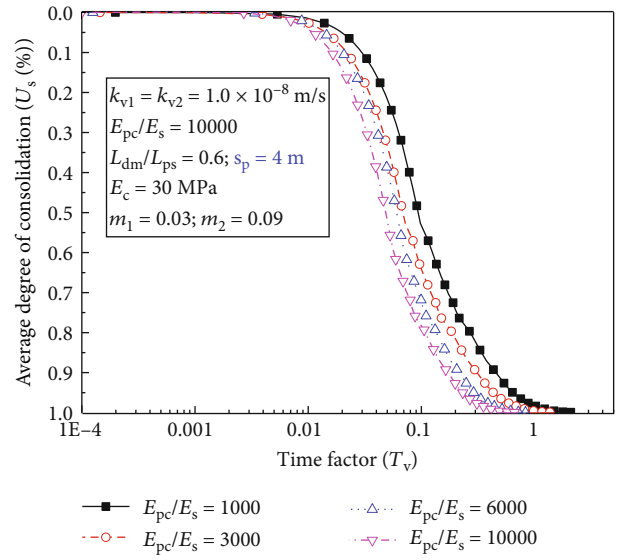

Figure 10: Effect of E_{pc}/E_s on the consolidation rate.

4.4. Effect of E_{pc}/E_s. Figure 10 illustrates the variations of U_s and T_v for the different the inner core-subsoil modulus ratio (E_{pc}/E_s). E_{pc} consists of 3 GPa, 3 GPa, 18 GPa, and 30 GPa, and E_s adopted the constant value of 3 MPa. The corresponding E_{pc}/E_s includes 1500, 3000, 6000, 30000, and 60000. It can be seen that the average consolidation rate increases as E_{pc}/E_s increases with a decreasing growth rate. The reason is that the larger the consolidation coefficient, the higher the consolidation rate. Besides, the equivalent consolidation coefficient increasing with E_{pc}/E_s affects the consolidation rate.

4.5. Effect of E_c/E_s. The PCCS piercing value and the composite compression modulus of Region A are both influenced by the stiffness of the cushion. U_s and T_v for the different the cushion-subsoil modulus ratio (E_c/E_s) are shown in Figure 11, where E_c consists of 0, 3 MPa, 15 MPa, and 30 MPa keeping E_s constant as 3 MPa. The corresponding E_c/E_s includes 1, 5, 10, and 15. The case with E_c/E_s of 1 indicates that no cushion was arranged on the surface of the CCF. It can be seen that the average degree of consolidation increases slightly with E_c/E_s and the growth rate decreases with E_c/E_s. The effect of E_c/E_s on the consolidation rate is less obvious than that of E_{pc}/E_s on the consolidation rate because of the smaller range of E_c/E_s. The consolidation rate

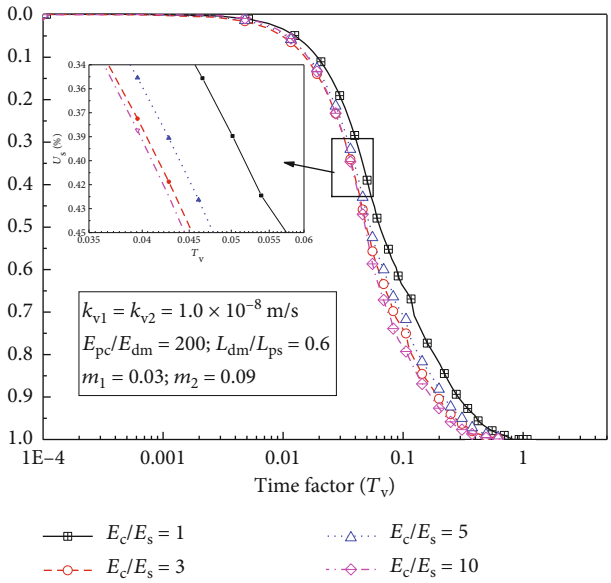

Figure 11: Effect of E_c/E_s on the consolidation rate.

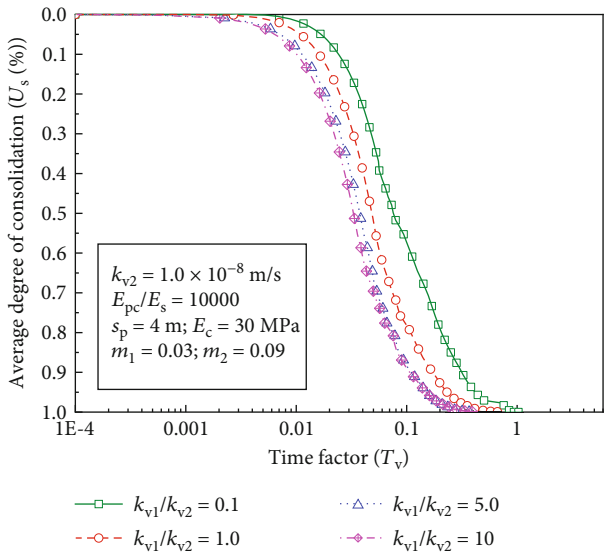

Figure 12: Effect of k_{v1}/k_{v2} on the consolidation rate.

for the CCF untreated with gravel cushion ($E_c/E_s = 1$) is lower than that for the CCF with the cushion. Without the gravel cushion, the soil around the piles needs to bear more loads and generates larger excess pore pressure, which takes longer time to dissipate.

4.6. Effect of k_{v1}/k_{v2}. Figure 12 presents the effect of the permeability coefficient ratio of the surrounding soil in Region A and Region B, (k_{v1}/k_{v2}) on consolidation characteristic, where k_{v1} consists of 10^{-9} m/s, 10^{-8} m/s, 5×10^{-8} m/s, and 10^{-7} m/s, keeping k_{v2} constant as 10^{-8} m/s. The corresponding k_{v1}/k_{v2} comprises 0.5, 1, 5, and 10. The consolidation rate increases as k_{v1} increases with a decreasing growth rate. Since the CCF reinforced with penetrated PCCSs and floating DM columns is simplified as double-layer ground whose permeability is reflected by the value of k_{v1}/k_{v2}, the larger k_{v1}/k_{v2} indicates the higher permeability of the subsoil to accelerate the consolidation of the surrounding soil.

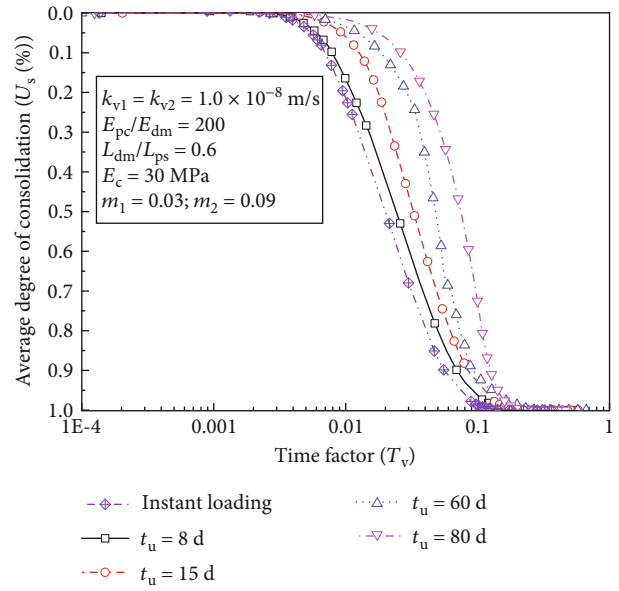

Figure 13: Influence of T_{vtc} on the average degree of consolidation.

4.7. Effect of t_u. The effect of the loading time (t_u) on the consolidation of this CCF is investigated by varying t_u from 60 d to 8 d, 30 d, 80 d, and 0 d in Figure 13. The case of t_u as 0 d can be regarded as instant loading. It can be seen from Figure 13 that the average consolidation rate of the CCF decreases with t_u. Since the additional stress increment increases with time and remains constant until t_u, the longer the loading period, the longer the time it takes for excess pore pressure to accumulate and dissipate.

5. Conclusion and Limitation

In order to give full play to the merits of different pile techniques, the CCF reinforced with penetrated PCCSs and floating DM columns is proposed. Based on an idealized double-layered consolidation model and modified equal-strain assumptions, an analytical method for the consolidation of this CCF is derived. Besides, the average consolidation degree predicted from this analytical solution is verified by that obtained from numerical analysis. Finally, a parametric study is carried out to analyze the effect of key factors on consolidation of this CCF. The following conclusions can be drawn:

(1) The equivalent compressive moduli of $E_{comp1}/(1 - m_1 - m_2)$ and $E_{comp2}/(1 - m_1)$ of the surrounding soil in Region A and Region B, respectively, are larger than that of the untreated-soil ground. Therefore, the consolidation rate of this CCF can be much faster than that of the natural ground

(2) The theoretical values of consolidation rate are slightly bigger than the numerical ones for $t > t_u$. The reason is that the nonlinear variation of the additional stress of subsoils assumed in the numerical simulation is different from that assumed to vary linearly along with the depth in the analytical method

(3) The average consolidation rate of this CCF is mainly affected by E_{pc} and m_1 because of the PCCSs penetrating the soft soils. m_2 has limited effect on the consolidation rate of this CCF induced by the floating effect of the DM columns

(4) The average consolidation rate is improved slightly with E_{pc}/E_s and E_c/E_s in this CCF. The average consolidation rate decreases with t_u. The consolidation rate increases as k_{v1}/k_{v2} increases with a decreasing growth rate. Besides, the consolidation rate of this CCF with the gravel cushion is higher than that of the CCF without the gravel cushion. The consolidation rate of the CCF reinforced with penetrated PCCSs and DM columns increases obviously compared with the traditional CCF improved by PC piles united with DM columns

(5) The additional stress of subsoils in the analytical method was simplified as the linear variation along with the depth, which may be different from that in situ. The further research will be conducted to improve the current method

Data Availability

The data used to support the findings of this study are available from the corresponding author upon reasonable request.

Conflicts of Interest

The authors declare that they have no conflicts of interest.

Acknowledgments

This work is funded by the National Natural Science Foundation of China (nos. 42277146 and 52078129) and the Natural Science Foundation of Jiangsu Province of China (grant no. BK20210051). All of these financial supports are gratefully acknowledged.

References

[1] C. Yu, A. Zhang, Y. Wang, and W. Ren, "Analytical solution for consolidation of combined composite foundation reinforced with penetrated impermeable columns and partially penetrated permeable stone columns," *Computers and Geotechnics*, vol. 124, article 103606, 2020.

[2] T. Yang, J. Z. Yang, and J. Ni, "Analytical solution for the consolidation of a composite ground reinforced by partially penetrated impervious columns," *Computers and Geotechnics*, vol. 57, pp. 30–36, 2014.

[3] M. M. Lu, K. H. Xie, S. Y. Wang, and C. X. Li, "Analytical solution for the consolidation of a composite foundation reinforced by an impervious column with an arbitrary stress increment," *International Journal of Geomechanics*, vol. 13, no. 1, pp. 33–40, 2013.

[4] F. Lai, D. Yang, S. Liu, H. Zhang, and Y. Cheng, "Towards an improved analytical framework to estimate active earth pressure in narrow c-ϕ soils behind rotating walls about the base," *Computers and Geotechnics*, vol. 141, article 104544, 2022.

[5] P. Jia, A. Khoshghalb, C. Chen, W. Zhao, M. Dong, and E. G. Alipour, "Modified Duncan-Chang constitutive model for modeling supported excavations in granular soils," *International Journal of Geomechanics*, vol. 20, no. 11, article 04020211, 2020.

[6] M. Y. Fattah and W. H. S. Al-Soudani, "Bearing capacity of closed and open ended pipe piles installed in loose sand with emphasis on soil plug," *Indian Journal of Geo-Marine Sciences*, vol. 5, pp. 703–724, 2016.

[7] F. Lai, N. Zhang, S. Liu, and D. Yang, "A generalised analytical framework for active earth pressure on retaining walls with narrow soil," *Géotechnique*, pp. 1–16, 2022.

[8] J. Han, "Recent research and development of ground column technologies," *Proceedings of the Institution of Civil Engineers-Ground Improvement*, vol. 168, no. 4, pp. 246–264, 2015.

[9] R. Lang and A. Yang, "A quasi-equal strain solution for the consolidation of a rigid pile composite foundation under embankment loading condition," *Computers and Geotechnics*, vol. 117, article 103232, 2020.

[10] Y. Chen, W. Zhao, J. Han, and P. Jia, "A CEL study of bearing capacity and failure mechanism of strip footing resting on _c_ - _φ_ soils," *Computers and Geotechnics*, vol. 111, pp. 126–136, 2019.

[11] M. Bouassida, M. Y. Fattah, and N. Mezni, "Bearing capacity of foundation on soil reinforced by deep mixing columns," *Geomechanics and Geoengineering*, vol. 17, no. 1, pp. 309–320, 2022.

[12] J. J. Zheng, Y. Liu, and Z. J. Xu, "Reliability-based design applied to multi-column composite foundations," in *Advances in Ground Improvement*, Orlando, Florida, United States, 2009.

[13] T. Yang, Y. Ruan, J. Ni, and C. Li, "Consolidation analysis of an impervious multi-pile composite ground under rigid foundation," *European Journal of Environmental and Civil Engineering*, vol. 25, no. 7, pp. 1287–1301, 2021.

[14] L. Tong, H. Li, S. Ha, and S. Liu, "Lateral bearing performance and mechanism of piles in the transition zone due to pit-in-pit excavation," *Acta Geotechnica*, vol. 17, no. 5, pp. 1935–1948, 2022.

[15] M. Y. Fattah, W. H. Al-Soudani, and M. Omar, "Estimation of bearing capacity of open-ended model piles in sand," *Arabian Journal of Geosciences*, vol. 9, no. 3, 2016.

[16] M. Lu, H. Jing, A. Zhou, and K. Xie, "Analytical models for consolidation of combined composite ground improved by impervious columns and vertical drains," *International Journal for Numerical and Analytical Methods in Geomechanics*, vol. 42, no. 6, pp. 871–888, 2018.

[17] T. Lu, G. Zhang, S. Liu, B. Zheng, and X. Zhang, "Numerical investigation of the temperature field and thermal insulation design of cold-region tunnels considering airflow effect," *Applied Thermal Engineering*, vol. 191, article 116923, 2021.

[18] Z. Zhang, F. Rao, and G. Ye, "Analytical modeling on consolidation of stiffened deep mixed column-reinforced soft soil under embankment," *International Journal for Numerical*

and Analytical Methods in Geomechanics, vol. 44, no. 1, pp. 137–158, 2020.

[19] A. Wang, D. Zhang, and Y. Deng, "Lateral response of single piles in cement-improved soil: numerical and theoretical investigation," *Computers and Geotechnics*, vol. 102, pp. 164–178, 2018.

[20] A. Wang, D. Zhang, and Y. Deng, "A simplified approach for axial response of single precast concrete piles in cement-treated soil," *International Journal of Civil Engineering*, vol. 16, no. 10, pp. 1491–1501, 2018.

[21] Z. Zhang, F. Rao, and G. Ye, "Design method for calculating settlement of stiffened deep mixed column-supported embankment over soft clay," *Acta Geotechnica*, vol. 15, no. 4, pp. 795–814, 2020.

[22] X. Wang, J. Zheng, and J. Yin, "On composite foundation with different vertical reinforcing elements under vertical loading: a physical model testing study," *Journal of Zhejiang University Science A*, vol. 11, no. 2, pp. 80–87, 2010.

[23] F. X. Yan and X. Z. Huang, "Experiment research of bearing behavior on lime-soil pile and CFG pile rigid-flexible pile composite subgrade," in *Ground Improvement and Geosynthetics*, Shanghai, China, 2014.

[24] J. J. Zheng, J. H. Ou, N. Z. Yuan, and Q. H. Fang, "Analytical solutions of composite modulus of multi-element composite foundation by parametric variational principle," *Chinese Jounal of Geotechnical Engineering*, vol. 25, pp. 317–321, 2003.

[25] J. Zheng, Y. Liu, Y. Pan, and J. Hu, "Statistical evaluation of the load-settlement response of a multicolumn composite foundation," *International Journal of Geomechanics*, vol. 18, no. 4, p. 18, 2018.

[26] G. Ye, Y. Cai, and Z. Zhang, "Numerical study on load transfer effect of stiffened deep mixed column-supported embankment over soft soil," *KSCE Journal of Civil Engineering*, vol. 21, no. 3, pp. 703–714, 2017.

[27] A. Wonglert, P. Jongpradist, P. Jamsawang, and S. Larsson, "Bearing capacity and failure behaviors of floating stiffened deep cement mixing columns under axial load," *Soils and Foundations*, vol. 58, no. 2, pp. 446–461, 2018.

[28] P. Voottipruex, P. Jamsawang, P. Sukontasukkul, P. Jongpradist, S. Horpibulsuk, and P. Chindaprasirt, "Performances of SDCM and DCM walls under deep excavation in soft clay: field tests and 3D simulations," *Soils and Foundations*, vol. 59, no. 6, pp. 1728–1739, 2019.

[29] P. Voottipruex, D. T. Bergado, T. Suksawat, P. Jamsawang, and W. Cheang, "Behavior and simulation of deep cement mixing (DCM) and stiffened deep cement mixing (SDCM) piles under full scale loading," *Soils and Foundations*, vol. 51, no. 2, pp. 307–320, 2011.

[30] C. Wang, Y. Xu, and P. Dong, "Plate load tests of composite foundation reinforced by concrete-cored DCM pile," *Geotechnical and Geological Engineering*, vol. 32, no. 1, pp. 85–96, 2014.

[31] A. Wonglert and P. Jongpradist, "Impact of reinforced core on performance and failure behavior of stiffened deep cement mixing piles," *Computers and Geotechnics*, vol. 69, pp. 93–104, 2015.

[32] W. Raongjant and M. Jing, "Field testing of stiffened deep cement mixing piles under lateral cyclic loading," *Earthquake Engineering and Engineering Vibration*, vol. 12, no. 2, pp. 261–265, 2013.

[33] C. Wang, Y. Xu, and P. Dong, "Working characteristics of concrete-cored deep cement mixing piles under embankments," *Journal of Zhejiang University Science A*, vol. 15, no. 6, pp. 419–431, 2014.

[34] C. Cheng, P. Ni, W. Zhao et al., "Face stability analysis of EPB shield tunnel in dense sand stratum considering the evolution of failure pattern," *Computers and Geotechnics*, vol. 130, article 103890, 2021.

[35] Y. Chen, P. Ni, J. Han, W. Zhao, P. Jia, and W. Zheng, "Stress distribution of embedded caisson foundation under lateral load based on the continuum approach," *Marine Georesources & Geotechnology*, vol. 40, pp. 1328–1340, 2022.

[36] Z. Chen, P. Ni, Y. Chen, and G. Mei, "Plane-strain consolidation theory with distributed drainage boundary," *Acta Geotechnica*, vol. 15, no. 2, pp. 489–508, 2020.

[37] X. Zheng, L. Wang, and Y. Xu, "Analytical solutions of 1-D chemo-hydro-mechanical coupled model of saturated soil considering osmotic efficiency," *International Journal for Numerical and Analytical Methods in Geomechanics*, vol. 45, no. 17, pp. 2522–2540, 2021.

[38] J. Castro and C. Sagaseta, "Consolidation around stone columns. Influence of column deformation," *International Journal for Numerical and Analytical Methods in Geomechanics*, vol. 33, no. 7, pp. 851–877, 2009.

[39] K. Deb and A. Behera, "Rate of consolidation of stone column-improved ground considering change in permeability and compressibility during consolidation," *Applied Mathematical Modelling*, vol. 48, pp. 548–566, 2017.

[40] J. Castro and C. Sagaseta, "Deformation and consolidation around encased stone columns," *Geotextiles and Geomembranes*, vol. 29, no. 3, pp. 268–276, 2011.

[41] C. Jorge and S. César, "Consolidation and deformation around stone columns: numerical evaluation of analytical solutions," *Computers and Geotechnics*, vol. 38, no. 3, pp. 354–362, 2011.

[42] H. Li, S. Liu, and L. Tong, "A numerical interpretation of the soil-pile interaction for the pile adjacent to an excavation in clay," *Tunnelling and Underground Space Technology*, vol. 121, article 104344, 2022.

[43] S. W. Abusharar, J. Zheng, and B. Chen, "Finite element modeling of the consolidation behavior of multi-column supported road embankment," *Computers and Geotechnics*, vol. 36, no. 4, pp. 676–685, 2009.

[44] K. Xie, "Theory of one dimensional consolidation of double-layered ground and its applications," *Chinese Journal of Geotechnical Engineering*, vol. 16, no. 5, pp. 24–35, 1994.

[45] C. Zhang, S. Liu, D. Zhang, F. Lai, T. Lu, and Y. Liu, "A modified equal-strain solution for consolidation behavior of composite foundation reinforced by precast concrete piles improved with cement-treated soil," *Computers and Geotechnics*, vol. 150, article 104905, 2022.